AL-QADISIYAH JOURNAL FOR ENGINEERING SCIENCES 13 (2020) 125–135

Contents lists available at http://qu.edu.iq

Al-Qadisiyah Journal for Engineering Sciences

Journal homepage: http://qu.edu.iq/journaleng/index.php/JQES

Optimization of process parameters for the electrochemical oxidation treatment of petroleum refinery wastewater using porous graphite anode

Ahmad S. Fahim [a], Ali H. Abbar [a]*

[a] *Chemical Engineering Department -Faculty of Engineering – University of Al-Qadisiyah-Iraq.*

ARTICLE INFO

Article history:
Received 01 April 2020
Received in revised form 17 May 2020
Accepted 25 June 2020

Keywords:
Petroleum refinery wastewater
Indirect oxidation
Porous graphite
Response surface methodology
COD removal

ABSTRACT

The present paper deals with the electrochemical treatment of wastewaters generated from Al-Diwaniyah petroleum refinery plant in a batch electrochemical reactor using stainless steel cathode and porous graphite anode. Effects of operating parameters such as current density (5-25 mA/cm^2), pH (3-9), addition of NaCl (0-2g/l), and time (20–60 min) on the removal efficiency of chemical oxygen demand (COD) were investigated. The results revealed that both pH and NaCl addition have the main effect on the COD removal efficiency confirming that the system was governed by reaction conditions in the bulk of solution not upon the electro oxidation of chloride ion on the surface of the electrode. Parametric optimization was carried out using Response Surface Methodology (RSM) combined with Box–Behnken Design (BBD) to maximize the removal of COD. Under optimized operating conditions of initial pH: 3, current density = 25 mA/cm^2, NaCl conc. = 2 g/l, and time = 60 min, the removal efficiency of COD was found to be 98.16% with energy consumption of 9.85 kWh/kgCOD which is relatively lower than the previous works.

1. Introduction

In Petroleum refinery process, crude oil converts into its main fractions using physical, thermal, and chemical separation processes then these fractions are further processed through a series of other conversion and separation steps into final petroleum products such as gasoline, Liquefied Petroleum Gas (LPG), diesel fuels, kerosene, lubrication oils, and many others. For the purpose of getting these products, a large quantity of fresh water is utilized for refinery processes, mainly for hydro-treating, distillation, desalting, and cooling systems [1]. About 80-90 % of the water used in petroleum refinery process converts into wastewater. Diya'uddeen et al. [2] identified that the quantity (as volume) of the effluents generated from petroleum refinery in the course of crude oil processing is 0.4–0.6 times the quantity (as volume) of the crude oil processed.

The composition of generated wastewaters depends on the type of oils, mode of manufacturing, and process configuration. The polluted wastewater generated by refineries contain COD levels of nearly 300–600 mg/L; phenol concentration of 20–200 mg/L; benzene concentration of 1–100 mg/L; heavy metals with concentrations as chrome (0.1–100 mg/L), as lead (0.2–10 mg/L), and other pollutants [3]. Direct disposal of these wastewaters could lead to essential pollution problems for the environment

* *Corresponding author.*
E-mail address: : ali.abbar@qu.edu.iq (Ali H. Abbar)

https://doi.org/10.30772/qjes.v13i2.652

Nomenclature

Adj. MS	Adjusted mean of the square	OFAT	One-factor-at-a-time
adj. R^2	Adjusted coefficient of multiple correlation	PI	Prediction interval
Adj. SS	Adjusted sum of the square	pred. R^2	Predicted multiple correlation coefficient
a_i	The first-class(linear) major effect	Pt	Platinum
a_{ii}	Second-class major effect	RE	Removal Efficiency (%)
a_{ij}	The interaction effect	RSM	Response surface methodology
ANOVA	Analysis of variance	S	Standard Error of the Regression
a_o	The intercept term	SE	Standard error of mean
BBD	Box–Behnken Design	Seq. SS	Sum of square
BDD	Boron Doped diamond	t	time , min
CI	Confidence interval	T.D.S	Total dissolved solids
COD	Chemical oxygen demand	V	Volume of the effluent (L)
Cp	Reiterated number of the central point	X1	Current density ,m A/cm^2
Cr. %	Percentage contribution for each parameter	*x1*	coded value of current density
D_F	The desirability function	X2	pH
DOF	Degree of freedom	*x2*	coded value of pH
E	Voltage of cell, Volt	X3	NaCl addition (g/l)
EC	Energy Consumption, kWh / kg COD	*x3*	coded value of NaCl addition
EO	Electrochemical oxidation	X4	Time(min)
F	Faraday Constant , A s mol^{-1}	*x4*	coded value of Time
I	Current applied , A	XRD	X-Ray Diffraction
k	Number of process variables	Y	Represents the dependent variable (RE)
N	Number of runs		

due to the high content of polycyclic aromatic compounds that have very toxic effects on the environment since they have the ability to exist in the environment for a long time. Therefore, these effluents should be treated before discharging [4].

The common treatment method of wastewater generated from refinery plants is based on mechanical and physicochemical methods in addition to further processing by biological treatment in an integrated activated-sludge treatment unit. Several other treatment methods were studied by the researchers including photocatalytic oxidation [5], wet oxidation [6], photo-degradation [7], catalytic vacuum distillation [8], coagulation–flocculation [9], Fenton oxidation [10], adsorption [11], membrane [12], membrane bioreactor [13], and chemical precipitation [14]. Generally speaking, the main ideas of most of these methods are the conversion of pollutants from one medium to another with low efficiency [2].

Electrochemical Oxidation (EO) treatment as a competitive technology has been used for treating different kinds of industrial wastewaters like pulp and paper plants, distillery, tannery, and textile industry. EO destruction of wastewaters containing phenolic compounds, such as dyes, poly-aromatic organic compounds, arsenic, and sulfidic spent caustic is also reported in the literature [15-19]. The electrochemical oxidation method offers a clean and powerful method for the mineralization of organic contaminants in water. Great attention for this method has been attracted because of the several distinguishing benefits such as versatility, safety, selectivity, energy efficiency, cost effectiveness, amenability to automation, and environmental compatibility since the main reagent used is the electron [20-22]. In contrast to chemical or photochemical oxidation, electrochemical oxidation does not need to utilize or store dangerous substances and its scale-up is more feasible [22]. During an electrochemical oxidation process, contaminants can be degraded by direct or indirect oxidation routes. In a direct route, the organic pollutants are first adsorbed on the surface of the anode and then destroyed by direct electron transfer. The indirect route includes the generation of strong oxidants electrochemically like hypochlorite/chlorine, hydrogen peroxide, and ozone, which react with the organic pollutants in the bulk solution [23]. Chloride is specifically attractive for using in the indirect oxidation due to the usually existing of chloride salts in wastewaters [24]. Furthermore, the role of active chlorine in the destruction of dyes and other organic compounds has been extensively studied by researchers in literature [25, 26]. Adding chloride ions to the effluent will also lead to minimize the energy consumption because of the improving in current efficiency and oxidation kinetics as well as decreasing the cell potential [27].

The performance of electrochemical oxidation processes in the destruction of contaminants is recognized by the complex interaction of different factors that may be optimized to get an economical and effective process. The main factors that determine the performance of an electrochemical oxidation process are: current density; electrode potential; mass transport regime; current distribution; conductivity; pH; cell design; electrode materials; and types of the contaminants. [28]. Hence, the electrochemical oxidation process seems to be a complex process due to the many variables affecting the mechanism of this process. In this case, the application of an experimental design method is essential to reduce the number of experiments with a better combination of the input factors. Statistical design decreases the process variability as well as the time required for trial and error experiments [29]. RSM is a substantial subject in the statistical design of experiments. It had been effectively applied in numerous processes for wastewater treatment like adsorption [30], chlorine disinfection [31], electrocoagulation [32], and Fenton-related process [33]. It is composed of a collection of mathematical and statistical approaches that could be used efficiently to analyze and model of many problems in which a response of interest is influenced by different parameters. The target of RSM is to evaluate the relative influence of different affecting parameters and finally obtain the best operating conditions by optimizing this response [34].

In spite of the electrochemical oxidation processes have plentiful applications for the treatment of several kinds of wastewater; their use for the treatment of wastewater generated from petroleum refinery plants is scarce in the literature. In previous works, the material of electrode is the key factor that determines the performance of an electrochemical oxidation process for the treatment of petroleum refinery effluents because of the material of electrode could change the mechanism of oxidation and anodic reactions. For example, Yavuz et al., [35] investigated the treatment of petroleum refinery wastewaters using direct and indirect electrochemical oxidation by two types of anodes; Boron Doped Diamond (BDD), and Ruthenium Mixed Metal Oxide (Ru-MMO). Yan et al., [36] used three dimensional porous graphite plate electrodes for treating of petroleum refinery wastewater using an EO process. Souza and Ruotolo [37] used Boron Doped Diamond anode (BDD), while Santos et al., [38] used Ti/RuO_2 anode in their works. Song and Ning [39] used ruthenium mixed

metal oxide electrode in the treatment of oil refinery effluents. Lately, Ghanim and Hamza [40] investigated the treatment of petroleum refinery wastewater using PbO_2 anode. All the above electrodes have many advantages and drawbacks depending on the type of oxidation and the composition of contaminants

The present study reports an indirect anodic oxidation process for treating a petroleum refinery wastewater generated from Al-Diwaniyah petroleum refinery plant using a porous graphite with a high specific surface area as an anode material and application the design of experiments as an optimization method. The process parameters were optimized by using Box-Behnken Design (BBD). The quadratic model has been developed in terms of input factors such as current density, initial pH, NaCl concentration, and time by performing the experiments based on the design matrix generated by RSM. This quadratic model was utilized for the assessment of parametric conditions that make COD removal maximum. No previous works have been conducted on the optimization of petroleum refinery wastewater using porous graphite anode. Selecting the porous graphite as anodic material is based on its availability, high specific area, and low cost in addition to its activity as anode materials in the indirect anodic oxidation [36].

2. 2. Experimental work

Petroleum refinery effluent samples were provided by Al-Diwaniyah petroleum refinery plant. Sample (40L) was collected from the feeding tank to the biological treatment unit and stored in closed containers at temperature 4 ºC until use. The characterization of this sample is shown in Table 1. Besides the properties of effluent taken from the settling tank of the final stage of the biological treatment unit that was measured by petroleum refinery plant administration with the permissible limit were mentioned in this table for comparison. The conductivity of raw water is 1.92 mS/cm which is low and resulted in increasing the cell potential, therefore supporting electrolyte should be used to increase the conductivity of the solution. Sodium sulfate (Na_2SO_4) at a concentration of 0.05 M was used as a supporting electrolyte which gives final conductivity of 12.9 mS/cm which is within the required range to obtain low cell potential [37].

Table 1. Characteristics of the effluents in Al-Diwaniyah petroleum refinery plant.

Test	Feed tank sample	Settling tank*	Permissible limit*
COD (mg/l)	590	65	100
pH	6.4	7.5	(6.9-9.5)
T.D.S	960	1680	…….
Cl^- (mg/l)	500	119	100
SO_4^{-2} (mg/l)	13.67	400	400
Turbidity(NTU)	28.49	6.44	41.3
Conductivity(mS/cm)	1.92	…..	……
Phenol(mg/l)	0.15	(0.01-0.05)	0.06

*provided by Al-Diwaniyah petroleum refinery plant administration.

A circular jacketed Perspex glass lab-scale batch electrochemical cell provided with Perspex cover was used for the anodic oxidation treatment experiments. It has dimensions (100 mm inside diameter with a length of 200 mm and thickness of 5mm) and an active electrolyte volume of 1.0 L. The jacket was made from Perspex and has external dimensions (130mm outside diameter with a length of 150 mm). The cover has external dimensions (130 mm outside diameter and thickness of 10 mm) and contains two slits for installing of electrodes and holes for inserting the probes of pH-meter and conductivity meter and sample taking out. A parallel plate configuration was adopted for the electrochemical reactor where stainless steel plate cathode (180 mm × 50 mm × 4 mm) and porous graphite anode (180 mm × 50 mm × 5 mm) were used. The distance between the cathode and the anode was fixed at 20 mm [40]. A digital direct current power supply (0–30 V, 0–5 A) Type (UNI-T, UTP3315PF) was used to provide constant current during each experiment (Galvanostatic mode). In each run, 1.0L solution was agitated using magnetic stirrer at a rotation speed of 500 rpm to achieve the proper mixing conditions then the required amount of the supporting electrolyte and NaCl (if needed) were added then mixing was continued at the same rotation speed during the experiment. All the experiments were carried out at constant temperature of 30 ±2 ºC using water bath (Memmert, type: WNB22, Germany). Fig.1 shows the schematic diagram of the electrochemical oxidation experimental setup supported by the required information. The electrolyte pH was measured using a digital pH meter (HNNA Instrument Inc.PH211, Romania) and the electrolyte acidity was adjusted using HCl or NaOH for appropriate experimental condition.

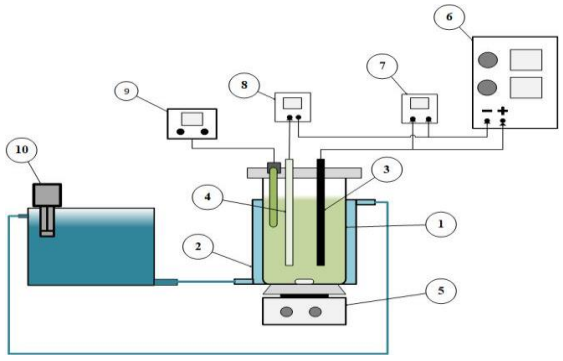

Figure 1. The schematic diagram of the experimental setup: 1) cell body, 2) jacket, 3) porous graphite anode, 4) cathode , 5) magnetic stirrer, 6) power supply, 7) voltmeter 8) Ammeter , 9) pH-meter, 10) water bath circulator

Conductivity and TDS were measured by using (HM digital Inc. model COM-100, Korea). Samples were taken and analysed to determine the COD and phenol concentration at the end of electrolysis.

The concentration of total organic compounds in the effluent is expressed in terms of (COD). Amount of COD in petroleum refinery effluents was measured by taken a sample (2ml) of effluent digested with $K_2Cr_2O_7$ as an oxidizing agent for 120 minutes at 150 °C in a COD thermos-reactor (RD125, Lovibond). The digested sample was cooled down to room temperature then analyzed in spectrophotometer (MD200, Lovibond). Phenol was measured by using Method 8047 assigned by Hach Company/Hach Lange GmbH, USA. Measuring of phenol concentration and COD were achieved three times and the average values were taken in this work.

2.1. Anode

Porous graphite is used as anode. It is a rectangular piece of graphite electrode with porosity 20-26% used for ARC furnace and supplied by Tokai Carbon Co., Ltd. Its structure was identified by using X-ray Diffractometer using Philips Analytical X-Ray B.V. with PC-APD,

Diffraction software, Philips expert, Holland). The X-Ray Diffraction (XRD) is operated at 40 kV and 30 mA with CuKα radiation as the X-ray source, λ=1.54056 Å. The scan step time was 0.5 sec with a step size of 0.02 degrees and a scan range of 10 – 99.99 degrees. The topography of graphite surface is investigated by means of Scanning Electron Microscopy (SEM) using Fesem Tescan Mira3, France. The measurement parameters were: AV = 15 kV, bias = 0, spot = 3.0 and HV = 2 kV, bias = 1400 V. The total surface area of graphite was measured by BET method using device (BET Tavana, Iran) provided with software based on micrometrics: MicroActive for TriStar II plus 2.03.

The COD removal efficiency was evaluated based on eq.1 [41]

$$RE\% = [(COD_i - COD_f)/COD_i] \times 100\% \quad (1)$$

Where RE% stands for the COD removal efficiency, COD_i represents the initial COD (mg L^{-1}), and COD_f is the final COD (mg L^{-1})

The energy consumption (EC) in any anodic oxidation represents the amount of the consumed energy in the process for a kilogram of COD that requires digesting. EC in (kWh/kg) may be acquired with the use of eq. 2 [42]:

$$EC = (E \times I \times t \times 1000)/((COD_i - COD_f) \times V) \quad (2)$$

Where EC represents the Energy Consumption (kWh/kg COD), E represents the measured cell voltage (Volt),I is the current (A), t represents the electrolysis time (h), COD_i and COD_f are the initial and final Chemical Oxygen Demand (mg/l), and V represents the volume of the effluent(L).

2.2. Design of experiments

Through application of mathematical and statistical collections, the relationship between a process response and its variables can be determined via adopting RSM [43]. In this study, the 3-level 4-factor Box–Behnken experimental design is employed to verify and check the factors that influenced on the removal of COD. Current density (X1) Initial pH (X2), NaCl concentration (X3), and time (X4) were taken as process variables, while the COD removal efficiency was taken as a response. The scales of process variables were coded as -1 (low level), 0 (middle or central point) and 1 (high level) [44]. Table 2 illustrates the process parameters with their chosen levels. Box–Behnken develops and improves the designs that needed for getting the suitable quadratic model with the required statistical properties though utilizing only a part of the required runs for a 3-level factorial. The number of runs (N) needed for carrying out of Box–Behnken design can be calculated by the following equation [45]:

$$N = 2k(k-1) + cp \quad (3)$$

Where k is the number of process variables and cp is the reiterated number of the central point. In this research, twenty seven runs were conducted for evaluating the impacts of the process variables on the COD removal efficiency. Table 3 illustrates the BBD proposed for the present research.

Table 2. Process variables with their level for refinery wastewater treatment

Process parameters	Rang in BOX-Behken design		
Coded levels	Low(-1)	Middle(0)	High(+1)
Xl-Current density (mA/cm^2)	5	15	25
X2- pH	3	6.5	10
X 3– NaCl addition (g/l)	0	1	2
X4- Time(min)	20	40	60

Table 3. Box- Behnken experimental design

Run	Blocks	Coded value				Real value			
		x_1	x_2	x_3	x_4	Current density (mA /cm^2) X1	pH X2	NaCl (g/l) X3	Time (min) X4
1	1	0	1	0	-1	15	10	1	20
2	1	0	-1	1	0	15	3	2	40
3	1	0	0	0	0	15	6.5	1	40
4	1	-1	0	0	-1	5	6.5	1	20
5	1	1	0	-1	0	25	6.5	0	40
6	1	0	-1	-1	0	15	3	0	40
7	1	1	1	0	0	25	10	1	40
8	1	1	0	0	1	25	6.5	1	60
9	1	0	0	1	-1	15	6.5	2	20
10	1	0	-1	0	1	15	3	1	60
11	1	1	0	1	0	25	6.5	2	40
12	1	0	0	-1	-1	15	6.5	0	20
13	1	0	0	-1	1	15	6.5	0	60
14	1	-1	1	0	0	5	10	1	40
15	1	-1	0	1	0	5	6.5	2	40
16	1	-1	0	-1	0	5	6.5	0	40
17	1	0	1	-1	0	15	10	0	40
18	1	0	-1	0	-1	15	3	1	20
19	1	0	0	0	0	15	6.5	1	40
20	1	1	0	0	-1	25	6.5	1	20
21	1	-1	-1	0	0	5	3	1	40
22	1	0	1	0	1	15	10	1	60
23	1	0	0	1	1	15	6.5	2	60
24	1	-1	0	0	1	5	6.5	1	60
25	1	0	1	1	0	15	10	2	40
26	1	1	-1	0	0	25	3	1	40
27	1	0	0	0	0	15	6.5	1	40

A second order polynomial model can be adopted based on BBD where fitting the interaction terms with the experimental data can be described by the following equation [46]:

$$\mathbf{Y=}\ a_0 + \sum a_i x_i + \sum a_{ii} x_i^2 + \sum a_{ij} x_i x_j \quad (4)$$

Where Y represents the Response Efficiency (RE), i and j are the index numbers for patterns, a_0 is intercept term, *x1, x2 ... x_k* are the process variables in coded form. a_i is the first-order(linear) main effect, a_{ii} second-order main effect and a_{ij} is the interaction effect. Analysis of variance was performed then the regression coefficient (R^2) was estimated to confirm the goodness of model fit.

3. Results and discussion

3.1. Characterization of anode

Figure 2 shows the XRD results of the porous graphite anode. It was coincided with the standard graphite structure having a reference code (96-901-2231) (blue) [47]. The graphite structure analysis shows a sharp diffraction peak at 2θ = 26.6255° with C (002) having a d-spacing of 3.34802Å. The SEM picture of porous graphite anode is shown in Figure 3 with magnification power (7500). It was found that the porous graphite has high porosity structure where large pores are formed which is different than the normal rigid graphite that possess smooth non-porous structure. BET

surface area of the porous graphite was found to be 22.7509 ± 0.5307 m^2/g which is higher than the BET of commercially available graphite felt (SGL carbon, GFA6 EA)(2.73 m^2/g) [48].

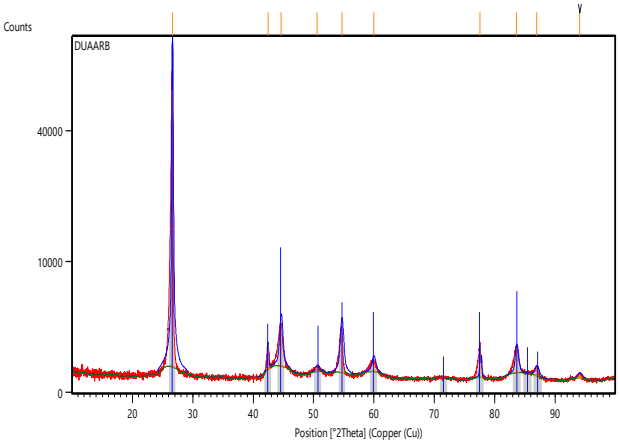

Figure 2. XRD Pattern of graphite

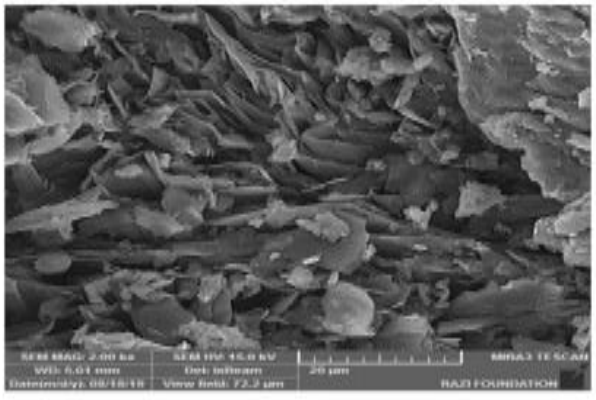

Figure 3. SEM image of porous graphite

3.2. Statistical analysis

For optimizing and studying the combined effects of the independent variables on the COD removal efficiency, twenty seven statistically designed batch runs were conducted for different combinations of process parameters. Table 4 shows the experimental results including COD Removal Efficiency (RE %) and Energy Consumption (EC).

It can be seen that COD removal efficiency is in the range of 54.98-98.80%. The energy consumption is in the range of (0.6-11.82) Kwh/kg COD. Minitab-17 software was used to analyse results of COD removal efficiency where an experimental relationship between COD removal efficiency and process parameters was obtained and formulated by the following quadratic model of COD Removal Efficiency (RE) in term of un-coded (real) units of process parameters (Eq.5):

$$RE\% = 61.4 + 0.030\,X1 - 2.99\,X2 + 16.99\,X3 + 0.176\,X4 + 0.0322\,(X1)^2 + 0.054\,(X2)^2 - 1.16\,(X3)^2 + 0.00374\,(X4)^2 + 0.0016\,X1*X2 - 0.070\,X1*X3 - 0.00471\,X1*X4 - 1.036\,X2*X3 + 0.0121\,X2*X4 + 0.0757\,X3*X4 \quad (5)$$

Table 4. Experimental results of Box–Behnken design for COD

Run	Blocks	Current density,(mA /cm^2)	pH	NaCl, (g/l)	Time, (min)	RE % Actual	RE % Predict	E, (Volt)	EC, (kwh/kg COD)
1	1	15	10	1	20	59.00	57.69	5.4	2.78
2	1	15	3	2	40	98.80	95.82	4.9	3.02
3	1	15	6.5	1	40	76.55	76.55	5.2	4.12
4	1	5	6.5	1	20	63.20	62.61	3.8	0.60
5	1	25	6.5	0	40	74.59	76.18	7.3	9.40
6	1	15	3	0	40	73.90	75.99	5.5	4.28
7	1	25	10	1	40	76.30	78.07	6.67	8.62
8	1	25	6.5	1	60	98.50	99.93	7.06	11.8
9	1	15	6.5	2	20	68.39	75.63	5.04	2.23
10	1	15	3	1	60	98.80	99.74	5.5	5.14
11	1	25	6.5	2	40	98.60	96.01	6.81	7.08
12	1	15	6.5	0	20	54.98	55.79	5.34	2.84
13	1	15	6.5	0	60	79.23	78.15	5.87	6.46
14	1	5	10	1	40	61.20	63.10	3.49	1.11
15	1	5	6.5	2	40	86.10	81.04	3.44	0.80
16	1	5	6.5	0	40	59.30	61.21	3.9	1.27
17	1	15	10	0	40	61.60	56.29	6.08	6.54
18	1	15	3	1	20	80.00	77.38	5.36	2.03
19	1	15	6.5	1	40	76.18	76.55	5.28	4.21
20	1	25	6.5	1	20	81.10	77.57	6.56	4.09
21	1	5	3	1	40	81.56	82.80	3.5	0.89
22	1	15	10	1	60	81.20	80.04	5.21	5.64
23	1	15	6.5	2	60	98.70	97.98	5.46	5.06
24	1	5	6.5	1	60	84.37	84.96	3.67	1.29
25	1	15	10	2	40	72.00	76.12	5.07	4.34
26	1	25	3	1	40	96.43	97.77	7.1	7.60
27	1	15	6.5	1	40	76.93	76.55	5.27	4.10

Where RE% is the response, i.e. COD removal efficiency, and X1, X2, X3and X4 are current density, pH, NaCl concentration, and Time respectively, where the variables X1X2, X1X3 , X1X4, X2X3, X2X4, X3X4 represent the interaction effect of all the parameters of the model. $(X1)^2$, $(X2)^2$, $(X3)^2$ and $(X4)^2$ are the measures of the main effect of variables current density, pH, NaCl concentration, and Time respectively.

Eq. (5) shows how the COD removal efficiency is affected by the individual variables (linear and quadratic) or double interactions. Values of positive coefficients revealed that the COD removal efficiency increased with the increasing of the related factors of these coefficients within the tested range while values of negative coefficients revealed the opposite effect. As can be seen current density, NaCl concentration, and Time were found to have a positive effect on the COD removal efficiency while pH has a negative effect. The results showed that effects of interactions are non-significant with a total contribution of (3.37%) from the model. The predicted values of the COD removal efficiency estimated from Eq.5 are also inserted in Table 4. The Box-Behnken design acceptability was recognized by using Analysis of Variance (ANOVA). For examine hypotheses on the factors of the model, ANOVA divides the total variation in a set of data into individual parts accompanied with specific sources of variation [49]. The acceptability of the model in ANOVA analysis is determined based on Fisher F-test and P-test. If the value of Fisher is large then most of the variation in the response can be illustrated by the regression equation. P-value is used for evaluating whether F is large enough to

recognize if the model is statistical significance. (90)% of the variability of the model could be clarified when a P-value lower than (0.05) [50].Table 5 illustrates ANOVA for the response surface model. In this table, degree of freedom (DF), sum of the square (SeqSS), percentage of contribution (Cr. %) for each parameter, adjusted sum of the square (Adj SS), adjusted mean of the square (Adj MS), F-value, and P-value were evaluated. F-value of (34.03) and P-value of (0.0001) were obtained which elucidating high significance for the regression model. The multiple correlation coefficient of the model was 97.54% conforming the regression is statistically significant and only (2.46) % of the total variations is not confirmed by the model. The adjusted multiple correlation coefficient (adj. R^2 = 94.68%) was in compatible with the predicted multiple correlation coefficient (pred. R^2=85.87%) in this model.

Results of Analysis of variance (ANOVA) showed that the percent of contribution of current density is (14.01 %) which is lower than other parameters. This means that the system is not controlled by current, meanwhile pH and concentration of NaCl have approximately the same significant effect on the process with contributions of 24.28%, 24.61% respectively. Time has the larger effect with contribution of 31.27 %. It is clear that contribution of both pH and NaCl concentration have the main effect on COD removal in the present work which means that the system is governed by reaction conditions in the bulk of solution not upon the electro oxidation of chloride ion on the surface of the electrode, i.e. the system is under bulk reaction control (reaction of chlorine with water) [51]. The linear term has the main contribution in the model with (94.17 %) followed by the square term with (1.91 %) as percent of contribution then 2-way interaction with a contribution of (1.46 %).

Table 5. Analysis of variance for COD removal

Source	DOF	Seq. SS	Cr.(%)	Adj. SS	Adj. MS	F-value	P-value
Model	14	4676.67	97.54	4676.67	334.05	34.03	0.001
Linear	4	4515.05	94.17	4515.05	1128.76	115.0	0.001
(X1)	1	671.85	14.01	671.85	671.85	68.45	0.001
(X2)	1	1164.07	24.28	1164.07	1164.07	118.6	0.001
(X3)	1	1179.89	24.61	1179.89	1179.89	120.2	0.001
(X4)	1	1499.24	31.27	1499.24	1499.24	152.8	0.001
Square	4	91.47	1.91	91.47	22.87	2.33	0.115
X1*X1	1	60.81	1.27	55.27	55.27	5.63	0.035
X2*X2	1	2.14	0.04	2.33	2.33	0.24	0.635
X3*X3	1	16.58	0.35	7.22	7.22	0.74	0.408
X4*X4	1	11.95	0.25	11.95	11.95	1.22	0.292
2-Way Inter.	6	70.15	1.46	70.15	11.69	1.19	0.374
X1*X2	1	0.01	0.001	0.01	0.01	0.00	0.971
X1*X3	1	1.95	0.04	1.95	1.95	0.20	0.664
X1*X4	1	3.55	0.07	3.55	3.55	0.36	0.559
X2*X3	1	52.56	1.10	52.56	52.56	5.36	0.039
X2*X4	1	2.89	0.06	2.89	2.89	0.29	0.597
X3*X4	1	9.18	0.19	9.18	9.18	0.94	0.353
Error	12	117.78	2.46	117.78	9.82		
Lack-of-Fit	10	117.50	2.45	117.50	11.75	83.55	0.012
Pure Error	2	0.28	0.01	0.28	0.14		
Total	26	4794.45	100				
Model summary		S	R^2	R^2(adj.)	Press	R^2(pred.)	
		3.1329	97.54%	94.68%	677.436	85.87%	

3.3. Effect of process variables on the COD removal efficiency

The interactive effect of the selected variables and their effect on the response is assessed via a graphical representation of statistical optimization using RSM. Figures (4-a,4- b) show the effect of the initial pH on COD removal efficiency for various values of current density (5-25 mA/cm^2) at constant NaCl conc. (1g/l) and time (40min.). Figure (4-a) represents the response surface plot while figure (4-b) shows the corresponding contour plot. From surface plot, it is clear that, at current density (5 mA/cm^2), a sharply decreasing in COD removal efficiency occurs as the initial pH increased from 3 to 10. This effect of pH on removal efficiency is in agreement with previous works [40, 51]. This behaviour can be explained as at high pH the active chlorine is present as hypochlorite that is less strong oxidant towards organic species with respect to hypochlorous acid which is highly strong oxidant and it is the main species present at pH close to 2 [51]. At pH of 3, the results showed that COD removal efficiency is increased approximately exponentially with increasing of current density from 5 to 15 mA/cm^2. Similar observation was found when pH is 10. This behaviour of current density effect on COD removal is in agreement with previous work [37,38] and could be explained by an increase in current density would be led to higher generation of hypochlorous acid in acidic solution and hypochlorite in alkaline solution which favouring organic compounds degradation by the indirect oxidation process [38]. The corresponding contour plot confirms that value of the COD removal efficiency ⩾90% lies in a small area in which the current density ranged between 18.5-25 mA/cm^2 and pH in the range (3-5).

The effect of NaCl concentration (addition of NaCl) on the COD removal efficiency for different current density (5-25 mA/cm^2) at constant pH(6.5) and time (40min.) is shown in Figures (5-a,5-b). The response surface plot Fig. (5-a) shows that COD removal efficiency is linearly increased with increasing of NaCl concentration at current density 5mA/cm^2. Similar trend occurs at current density of 25 mA/cm^2. These results are in agreement with the results observed in the literature [40].The corresponding contour plot Fig.(5-b) confirms that value of the COD removal efficiency ⩾90% lies in a small area in which the current density ranged between 20-25 mA/cm^2 and addition of NaCl at concentration between (1.5-2.0 g/l). Figures (6-a,6-b) show the effect of time on the COD removal efficiency for various values of current density (5-25 mA/cm^2) at constant pH(6.5) and NaCl conc. (1g/l). Figure (6-a) shows that the COD removal efficiency is quickly increased with increasing of time at low value of current density. The same behaviour was observed as the current density reach to 25 mA/cm^2. These results are in agreement with the results observed in the literature [37, 38, 40]. The corresponding contour plot Fig. (6-b) confirms that value of the COD removal efficiency ⩾90% lies in a small area in which the current density ranged between 17.5-25 mA/cm^{2}and times in range of 45-60min. Therefore, application of RSM will lead to identify the feasible optimum values of the studied factors in addition to its role in giving valuable information on interactions between the factors. Figure 7 shows the interaction plot among process paramours for COD Removal Efficiency (RE %). It can be seen that no significant interactions among variables were observed.

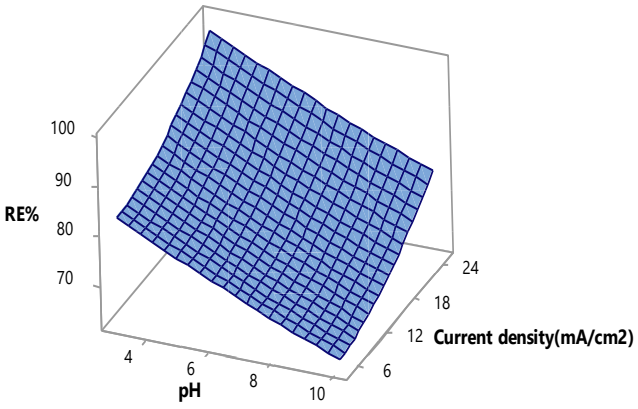

(a)

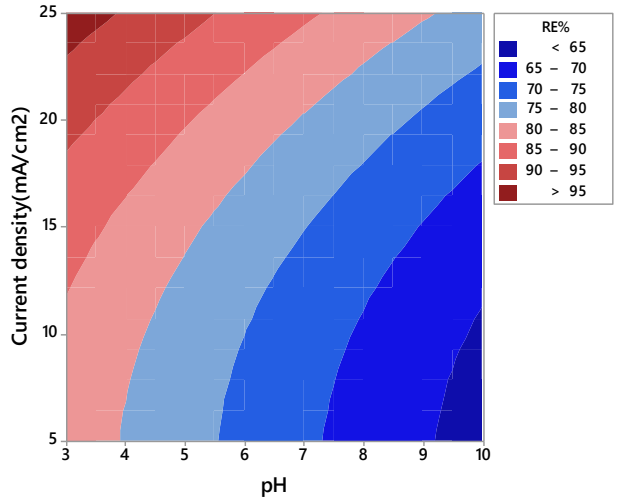

(b)

Figure 4. Response surface plot (a) and contour plot (b) for the impact of pH and current density on the COD (RE%)(Hold values NaCl=1g/l, time =40 min)

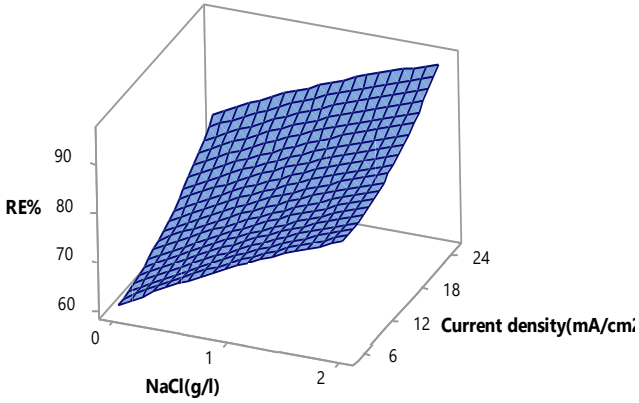

(a)

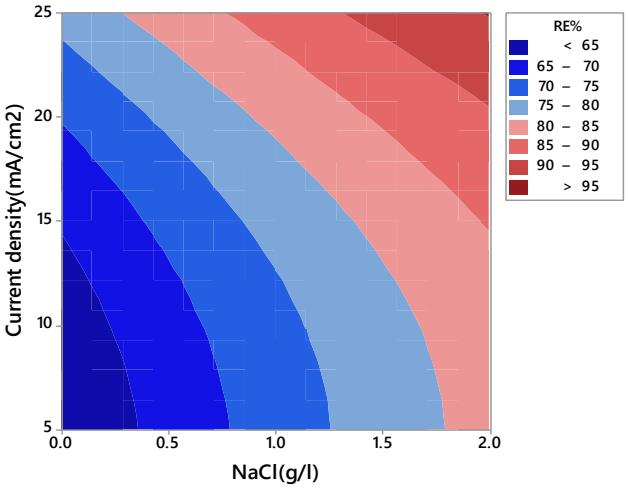

(b)

Figure 5. Response surface plot (a) and contour plot (b) showing the effect of NaCl concentration and current density on the COD removal efficiency (Hold values: pH=6.5, time=40min).

3.1. The optimization and confirmation test

To minimize energy losses and consequently treatment cost losses for any electrochemical removal system, optimization of its process conditions is essential and should be achieved. For optimizing the system, many criteria were identified to achieve the desired objective via maximizing the desirability function (D_F) through adjusting the weight or importance, which could alter the characteristics of an objective. The target fields for the variables have five options: none, maximize, minimize, objective and within the range. The goal of electrochemical removal of COD is designated as the 'maximum' with corresponding 'weight'1.0. The independent factors studied in this work were established within the range of the designed levels (current: 5-25 mA/cm^2, pH: 3-10, NaCl: 0-2g/l and time: 20-60 min.). The lower limit value of the COD removal efficiency was assigned at 54.98%, while the upper limit value was assigned at 98.8%. The optimization procedure was achieved under these boundaries and settings and the results are shown in Table 6 with the desirability function of (1). For their validation, two confirmative experiments were performed using the optimized parameters, the results are displayed in Table 7. After 60 min of the electrolysis, COD removal efficiency of 98.16% as an average value was achieved in pH=3 which is in compactable with the range of the optimum value getting from optimization analysis with desirability function of (1) (Table 6). Therefore, adopting Box–Behnken design in combined with desirability function is successful and efficient in optimizing COD removal using porous graphite anode. Additional experiment was conducted under the same optimum conditions with one exception that using initial pH of 7 instead of 3. The results show that COD removal efficiency in this case was 92.5% leading to a final COD level of

43ppm which is below the allowable limit determined by Al-Diwaniyah petroleum refinery plant administration (Table1). Table 8 shows a comparison between the properties of wastewater effluent and the treated effluent based on the present work. It can be seen that treated effluent has better properties and its properties are in agreement with the standard limits for discharging effluent (Table 1). COD removal efficiency of 98.8%, phenol removal efficiency of 99.6%, and turbidity removal efficiency of 95.65% base on the raw effluent properties were achieved in the present work confirming the activity of porous graphite anode in the indirect oxidation treatment of wastewater generated from Al-Diwaniyah petroleum refinery plant.

Table 6. Optimum of process parameters for maximum COD Removal Efficiency (RE %).

Response	Goal	Lower	Target	Upper	Weight	Importance
RE (%)	maximum	54.98	Maximum	98.8	1	1

Solution: Parameters				Results				
Current density (mA/cm^2)	pH	NaCl (g/l)	Time (min)	R E (%) Fit	D_F	SE Fit	95% CI	95% PI
25	3	2	60	111.785	1	4.79	(101.36; 122.21)	(99.32; 124.25)

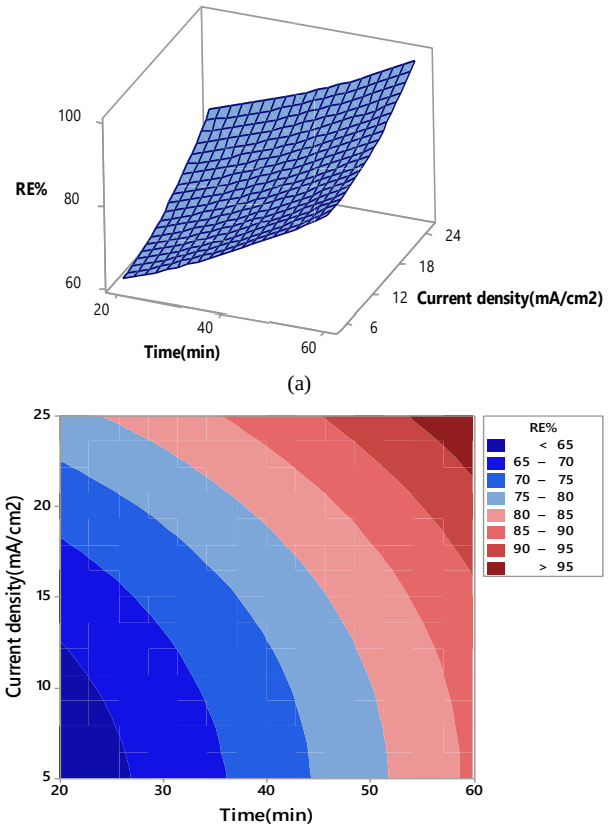

Figure 6. Response surface plot (a) and contour plot (b) showing the effect of time and current density on the COD removal efficiency (Hold values: NaCl=1g/l, pH=6.5).

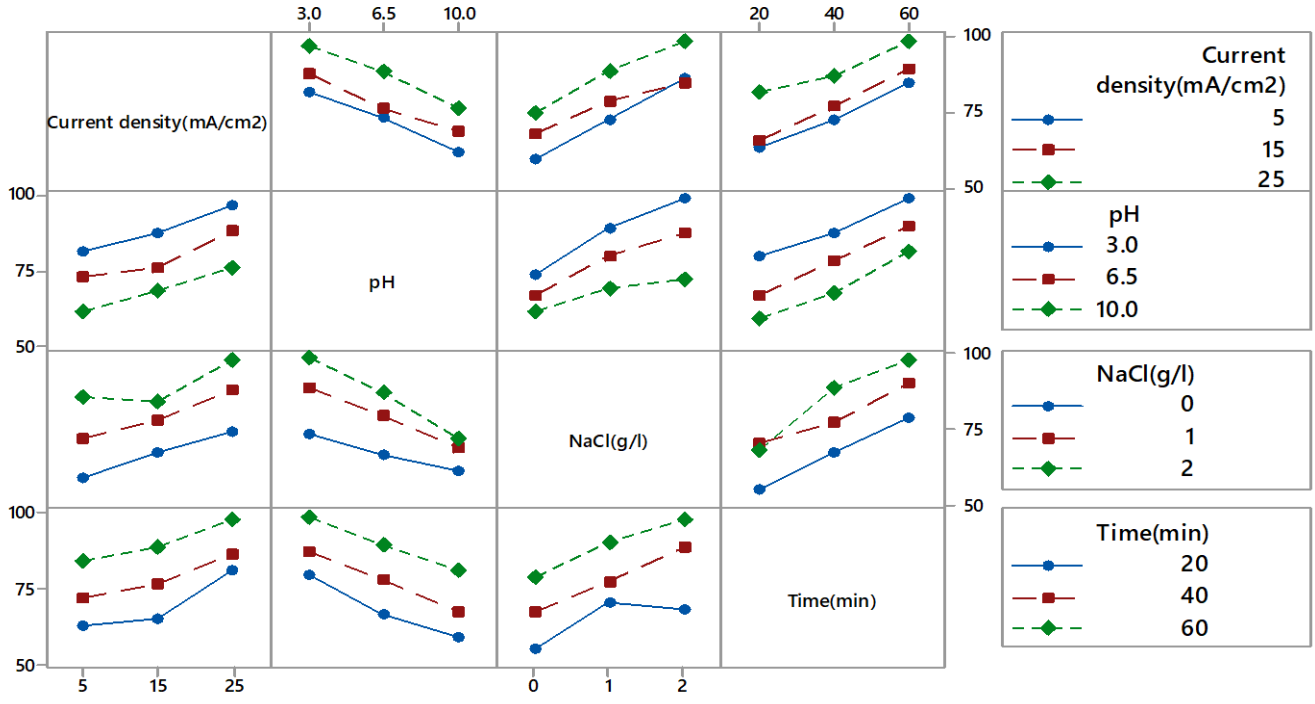

Figure 7. Interaction Plot for COD removal efficiency (RE %).

Table 7. Confirmative value of the optimum COD removal efficiency

Run	Current density ,(mA/cm^2)	pH	NaCl. (g/l)	Time ,(min)	E, (volt)	COD, (ppm) In	COD, (ppm) out	RE % Actual	RE % Average	EC. Kwh/kg COD
1	25	3	2	60	6.4	572	14	97.55	98.16	9.85
2	25	3	2	60	6.2	569	7	98.77		
3	25	7	2	60	6.0	585	43	92.65		9.68

Table 8. Comparison between the wastewater effluent and the treated effluent.

Parameter Effluent	COD (ppm)	Phenol (ppm)	Turbidity (NTU)	SO_4^{-2} (ppm)	Cl^- (g/l)
Raw effluent	590	0.15	28.49	13.67	0.5
Treated effluent	7 (98.8%)	0.0006 (99.6%)	1.24 (95.65%)	0.459	0.773

3.2. Comparison with previous works

The optimum conditions revealed that the indirect anodic oxidation of Al-Diwaniyah petroleum refinery could be performed using porous graphite anode with an initial COD (572 ppm) of wastewater where COD removal efficiency of 98.16% could be achieved at the end of an electrolysis time of 60 min. In this case an energy consumption of 9.85kWh/kg COD is required. In Table 9, we have given an extensive comparison between the present work with other related work for petroleum refinery wastewater degradation by indirect anodic oxidation process using different types of electrode under various conditions.

Table 9. Comparison of petroleum refinery wastewater degradation study using different type of electrode with literature under various conditions

Electrode type	COD	pH	Current density (mA/cm^2)	Time (min)	COD RE (%)	EC (kwh/ Kg COD)	Ref.
Porous Graphite	1021	6.5	12V	60	92.8	------	36
BDD	666	9.5	50	360	95		37
Ti/RuO_2	712	7.3	10	120	96	38.7	38
ruthenium mixed metal oxide	593	9	25	180	85	------	*39*
PbO_2	500	4	50	120	84.8	----	40
Porous Graphite	572	3	25	60	98.16	9.85	This work

It can be seen that the results of the present work are better than PbO_2 results. This is probably due to the high surface area of porous graphite that leads to liberation of more chlorine gas. Hence more reaction with H_2O leading to generation more HClO in acidic solution that degrades the organic compounds in wastewater. Comparison with work of Yan et al. [36] which used porous graphite anode is not conclusive since they operated at constant voltage not at constant current density as the case of present work. However their results are good in comparison with other works confirming the activity of porous graphite in oxidation of petroleum refinery wastewaters. Energy consumption in the present work is lower than that obtained by Santos et al. [38] work in spite of higher current density used in the present work.

4. Conclusions

The present research focused on investigating the effect of many operating parameters such as current density, initial pH, NaCl concentration, and time on the COD removal in the treatment of Al-Diwaniyah petroleum refinery wastewater using indirect anodic oxidation process on porous graphite anode and adopting Box-Behnken design as an optimization method. The experimental data were fitted to a second-order polynomial equation which was utilized for optimization of operating parameters. The optimum conditions were current density of 25 A/cm^2, NaCl concentration of 2g/l, pH equal to 3, and electrolysis time of 60 min, where COD removal efficiency of 98.16%, with energy consumption of 9.85 KWh/Kg COD were obtained. Results show that both pH and NaCl concentration have the main effect on COD removal in the present work which means that the system is governed by reaction conditions in the bulk of solution not on the electrooxidation reaction on the surface of electrode. This was in agreement with most mechanisms of the indirect anodic oxidation reaction reported in the literature.

Acknowledgment

The authors wish to acknowledge the helpful and technical assistance given by the staff of Chemical Engineering Department, College of Engineering- University of Al-Qadisiyah.

REFERENCES

[1] I. P. I. E. C. Association, Petroleum Refining Water/wastewater Use and Management: IPIECA Operations Best Practice Series, (2010).

[2] B. H. Diya'uddeen, W. M. A. W. Daud, and A. R. A. Aziz, Treatment technologies for petroleum refinery effluents: A review, Process safety and environmental protection, 89(2) (2011) 95–105.

[3] R. O. Ackermann *et al.*, Pollution prevention and abatement handbook 1998: toward cleaner production, (19128). The world bank, 1999.

[4] B. Mrayyan and M. N. Battikhi, Biodegradation of total organic carbons (TOC) in Jordanian petroleum sludge, Journal of hazardous materials, 120(1–3) (2005) 127–134.

[5] F. Shahrezaei, Y. Mansouri, A. A. L. Zinatizadeh, and A. Akhbari, Process modeling and kinetic evaluation of petroleum refinery wastewater treatment in a photocatalytic reactor using TiO2 nanoparticles, Powder Technology, 221 (2012) 203–212.

[6] Y. Sun, Y. Zhang, and X. Quan, Treatment of petroleum refinery wastewater by microwave-assisted catalytic wet air oxidation under low temperature and low pressure, Separation and purification technology, 62(3) (2008) 565–570.

[7] P. Stepnowski, E. M. Siedlecka, P. Behrend, and B. Jastorff, Enhanced photo-degradation of contaminants in petroleum refinery wastewater, Water Research, 36(9) (2002) 2167–2172.

[8] L. Yan, H. Ma, B. Wang, W. Mao, and Y. Chen, Advanced purification of petroleum refinery wastewater by catalytic vacuum distillation, Journal of hazardous materials, 178(1–3) (2010) 1120–1124.

[9] C. E. Santo, V. J. P. Vilar, C. M. S. Botelho, A. Bhatnagar, E. Kumar, and R. A. R. Boaventura, Optimization of coagulation–flocculation

and flotation parameters for the treatment of a petroleum refinery effluent from a Portuguese plant, Chemical Engineering Journal, 183 (2012) 117–123.

[10] A. R. A. Aziz and W. M. A. W. Daud, Oxidative mineralisation of petroleum refinery effluent using Fenton-like process, Chemical engineering research and design, 90(2) (2012) 298–307.

[11] M. H. El-Naas, S. Al-Zuhair, and M. A. Alhaija, Reduction of COD in refinery wastewater through adsorption on date-pit activated carbon, Journal of hazardous materials, 173(1–3) (2010) 750–757.

[12] E. Drioli and L. Giorno, Comprehensive membrane science and engineering, 1. Newnes, 2010.

[13] N. S. A. Mutamim, Z. Z. Noor, M. A. A. Hassan, and G. Olsson, Application of membrane bioreactor technology in treating high strength industrial wastewater: a performance review, Desalination, 305 (2012) 1–11.

[14] L. Altaş and H. Büyükgüngör, Sulfide removal in petroleum refinery wastewater by chemical precipitation, Journal of hazardous materials, 153(1–2) (2008) 462–469.

[15] M. Jović *et al.*, Electrochemical treatment of Reactive Blue 52 using zirconium, palladium and graphite electrode, CLEAN–Soil, Air, Water, 42(6) (2014) 804–808.

[16] P. Palo, J. R. Dominguez, J. Sánchez-Martín, and T. González, Electrochemical degradation of carbamazepine in aqueous solutions–optimization of kinetic aspects by design of experiments, CLEAN–Soil, Air, Water, 42(11) (2014) 1534–1540.

[17] J. Prakash Kushwaha, V. Chandra Srivastava, and I. Deo Mall, Studies on electrochemical treatment of dairy wastewater using aluminum electrode, AIChE journal, 57(9) (2011) 2589–2598.

[18] H. Olvera-Vargas, N. Oturan, D. Buisson, E. D. Van Hullebusch, and M. A. Oturan, Electro-Oxidation of the Pharmaceutical Furosemide: Kinetics, Mechanism, and By-Products, CLEAN–Soil, Air, Water, 43(11) (2015) 1455–1463.

[19] D. Maharana, J. Niu, N. N. Rao, Z. Xu, and J. Shi, Electrochemical degradation of triclosan at a Ti/SnO2-Sb/Ce-PbO2 anode, CLEAN–Soil, Air, Water, 43(6) (2015) 958–966.

[20] A. Anglada, A. Urtiaga, and I. Ortiz, Contributions of electrochemical oxidation to waste-water treatment: fundamentals and review of applications, Journal of Chemical Technology & Biotechnology, 84(12) (2009) 1747–1755.

[21] L. Fu *et al.*, Carbon nanotube and graphene oxide directed electrochemical synthesis of silver dendrites, Rsc Advances, 4(75) (2014) 39645–39650.

[22] L. Fu, G. Lai, and A. Yu, Preparation of β-cyclodextrin functionalized reduced graphene oxide: application for electrochemical determination of paracetamol, Rsc Advances, 5(94) (2015) 76973–76978.

[23] D. Rajkumar and J. G. Kim, Oxidation of various reactive dyes with in situ electro-generated active chlorine for textile dyeing industry wastewater treatment, Journal of hazardous materials, 136(2) (2006) 203–212.

[24] F. H. Oliveira, M. E. Osugi, F. M. M. Paschoal, D. Profeti, P. Olivi, and M. V. B. Zanoni, Electrochemical oxidation of an acid dye by active chlorine generated using Ti/Sn (1− x) Ir x O 2 electrodes, Journal of Applied Electrochemistry, 37(5) (2007) 583–592.

[25] M. Panizza and G. Cerisola, Electrocatalytic materials for the electrochemical oxidation of synthetic dyes, Applied Catalysis B: Environmental, 75(1–2) (2007) 95–101.

[26] D. Montanaro and E. Petrucci, Electrochemical treatment of Remazol Brilliant Blue on a boron-doped diamond electrode, Chemical Engineering Journal, 153(1–3) (2009) 138–144.

[27] I. D. Santos, J. C. Afonso, and A. J. B. Dutra, Behavior of a Ti/RuO2 anode in concentrated chloride medium for phenol and their chlorinated intermediates electrooxidation, Separation and purification technology, 76(2) (2010) 151–157.

[28] C. A. Martínez-Huitle and L. S. Andrade, Electrocatalysis in wastewater treatment: recent mechanism advances, Quimica Nova, 34(5) (2011) 850–858.

[29] W.-J. Chen, W.-T. Su, and H.-Y. Hsu, Continuous flow electrocoagulation for MSG wastewater treatment using polymer coagulants via mixture-process design and response-surface methods, Journal of the Taiwan Institute of Chemical Engineers, 43(2) (2012) 246–255.

[30] P. Sudamalla, P. Saravanan, and M. Matheswaran, Optimization of operating parameters using response surface methodology for adsorption of crystal violet by activated carbon prepared from mango kernel, Environ. Res, 22(1) (2012) 1–7.

[31] M. Umar, H. A. Aziz, and M. S. Yusoff, Assessing the chlorine disinfection of landfill leachate and optimization by response surface methodology (RSM), Desalination, 274(1–3) (2011) 278–283.

[32] D. Prabhakaran, C. A. Basha, T. Kannadasan, and P. Aravinthan, Removal of hydroquinone from water by electrocoagulation using flow cell and optimization by response surface methodology, Journal of Environmental Science and Health Part A, 45(4) (2010) 400–412.

[33] A. R. Khataee, M. Zarei, and L. Moradkhannejhad, Application of response surface methodology for optimization of azo dye removal by oxalate catalyzed photoelectro-Fenton process using carbon nanotube-PTFE cathode, Desalination, 258(1–3) (2010) 112–119.

[34] K. Thirugnanasambandham, V. Sivakumar, and M. J. Prakash, Treatment of egg processing industry effluent using chitosan as an adsorbent, Journal of the Serbian Chemical Society, 79(6) (2014) 743–757.

[35] Y. Yavuz, A. S. Koparal, and Ü. B. Öğütveren, Treatment of petroleum refinery wastewater by electrochemical methods, Desalination, 258(1–3) (2010) 201–205.

[36] L. Yan, H. Ma, B. Wang, Y. Wang, and Y. Chen, Electrochemical treatment of petroleum refinery wastewater with three-dimensional multi-phase electrode, Desalination, 276(1–3) (2011) 397–402.

[37] R. B. A. Souza and L. A. M. Ruotolo, Electrochemical treatment of oil refinery effluent using boron-doped diamond anodes, Journal of Environmental Chemical Engineering, 1(3) (2013) 544–551.

[38] I. D. Santos, M. Dezotti, and A. J. B. Dutra, Electrochemical treatment of effluents from petroleum industry using a Ti/RuO2 anode, Chemical engineering journal, 226 (2013) 293–299.

[39] S. Ye and N. Li, Comparison of electrochemical treatment of petroleum refinery effluents using electrooxidation, electrocoagulation and electrophenton process, Int. J. Electrochem. Sci, 11(7) (2016) 6173–6182.

[40] A. N. Ghanim and A. S. Hamza, Evaluation of Direct Anodic Oxidation Process for the Treatment of Petroleum Refinery Wastewater, Journal of Environmental Engineering (United States), 144(7) (2018) 1–8.

[41] O. Abdelwahab, N. K. Amin, and E. S. Z. El-Ashtoukhy, Electrochemical removal of phenol from oil refinery wastewater, Journal of hazardous materials, 163(2–3) (2009) 711–716.

[42] D. S. Ibrahim, C. Veerabahu, R. Palani, S. Devi, and N. Balasubramanian, Flow dynamics and mass transfer studies in a tubular electrochemical reactor with a mesh electrode, Computers & Fluids, 73 (2013) 97–103.

[43] M. A. Bezerra, R. E. Santelli, E. P. Oliveira, L. S. Villar, and L. A. Escaleira, Response surface methodology (RSM) as a tool for optimization in analytical chemistry, Talanta, 76(5) (2008) 965–977.

[44] M. Evans, Optimisation of manufacturing processes: a response surface approach, 791. Maney Pub, 2003.

[45] Y.-D. Chen, W.-Q. Chen, B. Huang, and M.-J. Huang, Process optimization of K2C2O4-activated carbon from kenaf core using Box–Behnken design, Chemical Engineering Research and Design, 91(9) (2013) 1783–1789.

[46] K. Yetilmezsoy, S. Demirel, and R. J. Vanderbei, Response surface modeling of Pb (II) removal from aqueous solution by Pistacia vera L.: Box–Behnken experimental design, Journal of Hazardous Materials, 171(1–3) (2009) 551–562.

[47] Z. Q. Li, C. J. Lu, Z. P. Xia, Y. Zhou, and Z. Luo, X-ray diffraction patterns of graphite and turbostratic carbon, Carbon, 45(8) (2007) 1686–1695.

[48] H. R. Jiang, W. Shyy, M. C. Wu, R. H. Zhang, and T. S. Zhao, A bi-porous graphite felt electrode with enhanced surface area and catalytic activity for vanadium redox flow batteries, Applied energy, 233 (2019) 105–113.

[49] L. Huiping, Z. Guoqun, N. Shanting, and L. Yiguo, Technologic parameter optimization of gas quenching process using response surface method, Computational Materials Science, 38(4) (2007) 561–570.

[50] J. Segurola, N. S. Allen, M. Edge, and A. Mc Mahon, Design of eutectic photoinitiator blends for UV/visible curable acrylated printing inks and coatings, Progress in Organic Coatings, 37(1–2) (1999) 23–37.

[51] O. Scialdone, S. Randazzo, A. Galia, and G. Silvestri, Electrochemical oxidation of organics in water: role of operative parameters in the absence and in the presence of NaCl, Water research, 43(8) (2009) 2260–2272.